CCFE
CULHAM CENTRE FOR FUSION ENERGY

UK Atomic Energy Authority

UKAEA-CCFE-PR(23)95

G. Pucella, E. Alessi, P. Buratti, M. V. Falessi, E. Giovannozzi, F. Zonca, M. Baruzzo, C. D. Challis, R. Dumont, D. Frigione, L. Garzotti, J. Hobirk, A. Kappatou, D. L. Keeling, D. King, E. Lerche, P. J. Lomas, M. Maslov, I. Nunes, F. Rimini, et al.

Experimental observation of beta-induced Alfven eigenmodes and geodesic acoustic modes during strong tearing activity in JET plasmas

Experimental observation of beta-induced Alfven eigenmodes and geodesic acoustic modes during strong tearing activity in JET plasmas

G. Pucella, E. Alessi, P. Buratti, M. V. Falessi, E. Giovannozzi, F. Zonca, M. Baruzzo, C. D. Challis, R. Dumont, D. Frigione, L. Garzotti, J. Hobirk, A. Kappatou, D. L. Keeling, D. King, E. Lerche, P. J. Lomas, M. Maslov, I. Nunes, F. Rimini, et al.

This is a preprint of a paper submitted for publication in
Plasma Physics and Controlled Fusion

Experimental observation of beta-induced Alfvén eigenmodes and geodesic acoustic modes during strong tearing activity in JET plasmas

G Pucella[1], E Alessi[2], P Buratti[1], M V Falessi[1], E Giovannozzi[1], F Zonca[1], M Baruzzo[1], C D Challis[3], R Dumont[4], D Frigione[5], L Garzotti[3], J Hobirk[6], A Kappatou[6], D L Keeling[3], D King[3], E Lerche[7], P J Lomas[3], M Maslov[3], I Nunes[8], F Rimini[3], P Sirén[9], C Sozzi[2], M F Stamp[3], Z Stancar[10], D Van Eester[7], M Zerbini[1], and JET Contributors*.

[1] ENEA, Fusion and Nuclear Safety Department, C.R. Frascati, Italy
[2] ISTP, Consiglio Nazionale delle Ricerche, Milano, Italy
[3] CCFE, Culham Science Centre, Abingdom, UK
[4] CEA, IRFM, Saint-Paul-lez-Durance, France
[5] Università degli Studi di Roma "Tor Vergata", Roma, Italy
[6] Max-Plank-Institute fur Plasmaphysik, Garching, Germany
[7] Laboratory for Plasma Physics-Ecole Royale Militaire, Brussels, Belgium
[8] IPFN/IST, University of Lisbon, Lisbon, Portugal
[9] VTT, Technical Research Centre of Finland, Espoo, Finland
[10] Slovevian Fusion Association, Ljubljana, Slovenia
* See the author list of E. Joffrin et al 2019 Nucl. Fusion 59 112021

E-mail: gianluca.pucella@enea.it

Abstract.

The experimental observation of multiple oscillations likely associated with beta-induced Alfvén eigenmodes with toroidal mode number $n = 1, 2$ during strong tearing activity in JET plasmas is reported in this work. It is found the frequencies of these oscillations range from 5 kHz to 20 kHz, being consistent with the low-frequency beta-induced gap opened, in the continuum of the shear Alfvén waves, by finite plasma compressibility. The conditions for excitation of those oscillations in JET plasmas without any fast particles population are investigated, indicating that a critical magnetic island size is indispensable. As main novelties compared to previous works, the observation of beta-induced Alfvén eigenmodes with $n = 2$ is reported for the first time, and the analysis of the electron temperature profiles from electron cyclotron emission shows the simultaneous presence of magnetic islands on different rational surfaces in pulses with multiple oscillations in the BAE frequency range. This observation supports the hypothesis of different BAE associated with different magnetic islands, with the value of the BAE frequencies generally scaling with the plasma temperature at the islands location, in agreement with the theoretical predictions. The occurrence of multiple oscillations at different frequencies is also observed in the landing phase of plasma pulses with locked tearing modes, where several relevant rational surfaces are present inside the plasma due to the high value of the safety factor at the edge. Some pulses, characterized by slowly rotating tearing modes, exhibit additional

oscillations with $n = 0$, likely associated with geodesic acoustic modes, which are one particular kind of zonal structures, and a bi-coherence analysis has confirmed a non-linear interaction among geodesic acoustic modes, beta-induced Alfvén eigenmodes and tearing modes.

1. Introduction

Beta-induced Alfvén eigenmodes (BAE) are shear Alfvén waves which can exist in the low-frequency beta-induced gap opened, in the continuum of the Alfvénic modes, thanks to coupling of the shear Alfvén wave with the compressional response of the plasma to the wave itself [1, 2, 3]. BAE need to be controlled in future burning plasma devices, such as ITER and DEMO, because the Alfvén dynamics of low-frequency and macroscopic scales may cause significant perturbations in the bulk of plasmas [4], leading to significant loss of energetic particles, which is penalizing for plasma heating and harmful for the reactor's first wall [5]. In this sense, BAE can be as deleterious as toroidal Alfvén eigenmodes (TAE) [6] to energetic particle confinement, and for this reason it is crucial to verify the agreement between theory and experiment in present-day tokamak plasmas. BAE were first observed in DIII-D and then in TFTR plasmas with fast ions [7, 8] and their excitation was explained in terms of interactions with the energetic particles; afterwards, BAE with fast ions were reported in Tore-Supra [9] and KSTAR [10] and in fast-electron plasmas in EAST tokamak [11]. However BAE were also observed in plasmas without any fast particles population during strong tearing mode (TM) activity [12], for the first time in FTU [13, 14] and TEXTOR [15] and afterwards on HL-2A [16] and J-TEXT [17]. The observation of BAE in plasmas without energetic particles induced to consider new excitation mechanisms, in particular the most promising non-linear excitation via three-wave coupling with a magnetic island sufficiently large to transfer enough energy to overcome Landau damping [3]. Multiple oscillations in the BAE frequency range have been observed in JET plasmas during strong TM activity, with the different frequency values likely associated with BAE coupled with different magnetic islands, and the excitation of BAE with toroidal number $n = 2$ is reported for the first time in this work.

Geodesic acoustic modes (GAM [18, 19, 20]), are a kind of zonal flow [21] with finite real frequency owing to the geodesic curvature of a toroidal magnetic field, driven by microscopic turbulence and supported by plasma compressibility in toroidal geometry. The GAM are mainly perceived as electrostatic fluctuations [22, 23, 24], although they also have a magnetic component which is created by the parallel return current [25, 26]. This component is second-order smaller than the electric one, therefore it is very difficult to observe in ohmic plasma. Nevertheless, in our observation, GAM are seen as $n = 0$ fluctuations in the magnetic spectrogram of pulses with both TM and BAE. It is worth noting that BAE and GAM have similar dispersion relations in the long-wavelength limit, when diamagnetic effects are ignored, even when finite Larmor radius corrections are accounted for [27]. The BAE/GAM degeneracy is expected to play an important role in the self-organized behaviors of burning plasmas, since their non-linear interplay via zonal structures is expected to be one of the dominant coupling mechanisms between the very disparate space-time scales of Alfvénic fluctuations and MHD modes on the one side and plasma turbulence on the other [27].

In the present work the conditions for BAE and GAM excitation in JET plasmas without fast particles are explored, looking at pulses where magnetic islands formed

by tearing instabilities grow up to large amplitudes and remain in those conditions for a relatively long time. Only pulses with rotating phases for magnetic islands are considered, to allow the estimation of the toroidal mode numbers. The main characteristics of the experimentally observed BAE are presented, pointing out the existence of a critical magnetic island size for the BAE excitation and a general scaling of the BAE frequencies with the plasma temperature at the islands location. The simulation of a real pulse with FALCON code [28] is performed to support the interpretation of the observed oscillations as BAE. The non-linear interaction among GAM, TM and BAE, firstly observed in HL-2A [29], is also investigated through spectral bicoherence analysis [30]. Finally the results are summarized and discussed.

2. Mode identification and theoretical framework

Tearing modes characterized by large magnetic islands are sometimes observed in different plasma scenarios at JET, both triggered by external events (reconnection processes, fishbone activities, perturbations associated with edge localized modes) and induced by an increased radiation emission from core or edge plasma. When tearing modes occur during the landing phase, characterized by the reduction of auxiliary heating and by the current ramp-down, the island growth can lead to a disruption [31]. In order to study the condition for BAE and GAM generation in JET plasma without fast particles and to investigate the characteristic of the related oscillations, we focused the attention on pulses with magnetic islands growing up to large amplitudes and remaining in those conditions for a relatively long time.

Time traces of some relevant quantities for a pulse characterized by the presence of the different oscillations we want to discuss in this work are shown in figure 1 (JPN 94446). In this pulse a progressive increase in the radiated power is observed, the neutral beam heating power starts to decrease at 12.0 s and the plasma current is ramped-down. A hollowing of the electron temperature profile takes place, as shown by the crossing of the time traces of the electron temperature near the magnetic axis and off-axis, respectively. This behavior is likely due to heavy impurity accumulation, which is a crucial point in JET with ITER-like wall [32]. Following the change in the temperature profile, a broadening of the current density profile is expected, as confirmed by the disappearance in the magnetic spectrogram of the $q = 1$ MHD activity, and a reconnection event at 12.7 s triggers $n = 2$ tearing modes, with magnetic islands that start rotating at 10 kHz and progressively slow down. In this phase, a real-time procedure is able to re-establish a peaked electron temperature profile providing central additional ion cyclotron resonance heating to counteract the inward transport of high-Z impurities [33, 34], and $n = 1$ activity reappears in the form of fishbones [35]. Finally, large and slowly rotating $n = 1$ tearing modes (detected by saddle coils) are triggered by sawtooth activity, without leading to disruption.

As it is possible to note from the magnetic spectrogram reported in figure 1, some additional oscillations are present with respect to the ones associated to $q = 1$, TM and

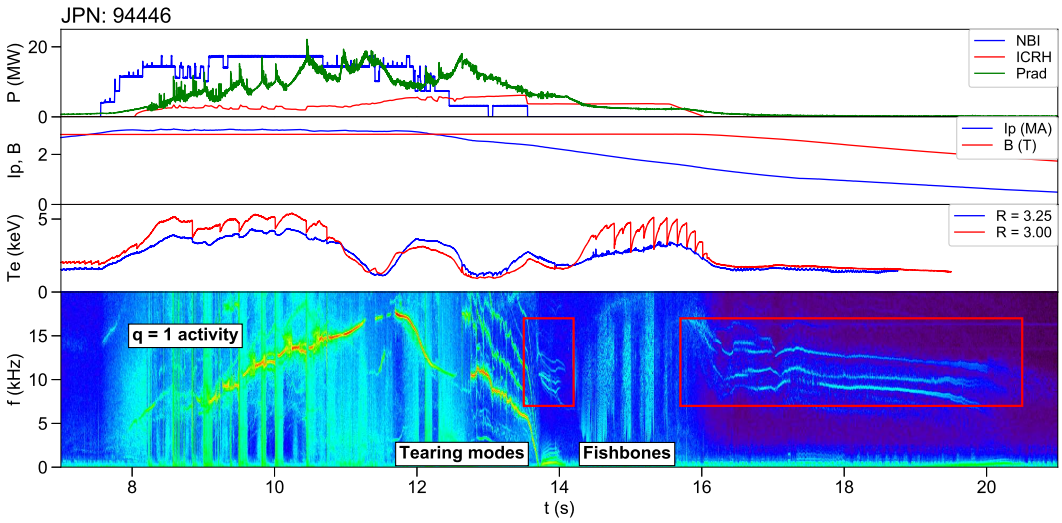

Figure 1. From top to bottom: neutral beam injected power, ion cycloctron resonance heating and radiated power; plasma current and toroidal magnetic field; electron temperature at different radii; spectrogram from a magnetic pick-up coil. JPN 94446.

fishbone activities, in the frequency range between 7 kHz and 17 kHz, as highlighted by two red boxes. The hypothesis we would like to support is that those additional oscillations sometimes observed in pulses with strong tearing activity are BAE and GAM. As a first remark, the observed frequency values are consistent with the low-frequency beta-induced gap, which is opened in the shear Alfvén continuous spectrum by finite plasma compressibility. In fact, ideal MHD theories [2] predict the frequency of the BAE is located in the gap:

$$0 < \left(\frac{\omega}{\omega_A}\right)^2 < \beta\gamma q^2 \tag{1}$$

where ω is the mode frequency, β is the ratio of kinetic and magnetic pressures, γ the ratio of specific heats, q the local safety factor, $\omega_A = v_A/qR_0$ the Alfvén frequency, R_0 the plasma major radius, $v_A = B/\sqrt{4\pi\rho}$ the Alfvén speed, B the magnetic field and ρ the plasma mass density. It is easy to see that the relevant BAE frequency range is ordered as the thermal ion transit frequency $\omega_{ti} = \sqrt{2T_i/m_i}/qR_0$, where T_i is the ion temperature in energy units and m_i is the ion mass ($\omega_A^2\beta \sim \omega_{ti}^2$). The result reported in equation (1) is also recovered as a specific (fluid) limit of the kinetic theory of low-frequency Alfvén modes presented in [3], where the following expression for γ in terms of the electron and ion temperature is obtained:

$$\gamma = \frac{7}{4} + \frac{T_e}{T_i} \tag{2}$$

so the upper limit of the BAE frequency gap in the Alfvén continuum, namely the so-called "continuum accumulation point" (CAP), is given by [3]:

$$\omega_{CAP} = \frac{1}{R_0}\sqrt{\frac{2T_i}{m_i}\left(\frac{7}{4} + \frac{T_e}{T_i}\right)} \tag{3}$$

This frequency is an upper bound for the BAE frequencies, so we can expect:

$$f_{BAE} = \alpha \frac{\omega_{CAP}}{2\pi} \tag{4}$$

with $\alpha < 1$. Concerning the possibility of GAM observation, our hypothesis is primarily supported by the fact that BAE and GAM have similar dispersion relations in the case of the long wavelength limit, namely the kinetic expression of the GAM dispersion relation can degenerate with that of the BAE [27]. A possible excitation mechanism of GAM in our pulses could be the non-linear interaction (i.e., three wave resonance) among GAM, BAE and strong TM.

A large dataset of pulses carried out on JET has been analyzed to highlight the excitation of BAE and GAM in pulses without any fast particles population (due to the reduction of the additional power). All the pulses carried out in the JET experimental campaigns C38, C38B and C38C (July 2019 - September 2020) in the so-called "baseline" [36] and "hybrid" [37] scenarios have been considered, resulting in 75 pulses where BAE and GAM activity were observed, corresponding to 11% of total pulses. A reduction of the dataset has been performed selecting only pulses with rotating phases for magnetic islands, to allow the estimation of the toroidal mode numbers, and additional pulses from other programs and/or experimental campaigns have been considered to clarify some specific aspects. The final dataset of 55 pulses has been divided in two subset referring to the beginning of the landing phase and to the late termination, respectively. Most of the 30 pulses selected in the beginning of the landing phase resulted to be carried out in the hybrid scenario, with flatter safety factor profiles and lower particle densities. A possible reason is that these conditions are more prone, with respect to high density plasmas with peaked electron temperature profiles, to develop large magnetic islands as a consequence of a temperature hollowing associated with core impurity accumulation, leading to a broadening of the current density profile [38, 39]. On the contrary, most of the 25 pulses selected in the late termination resulted to be carried out in the baseline scenario, which is characterized by a higher incidence of strong MHD activity in the termination phase. In these pulses, in addition to the triggers associated with sawtooth crashes, an increased radiation emission from core or edge plasma, leading to temperature hollowing and edge cooling, respectively, is observed before the onset of the modes in absence of a sawtooth trigger [40].

3. Excitation of BAE with toroidal number $n = 2$

The dynamics of the $n = 2$ TM triggered in JPN 94446 by the reconnection event at 12.7 s (see figure 1) and the correlation with additional oscillations in the spectrogram at higher frequencies are analyzed in detail in figure 2 (left). After the TM onset, mode analysis at the fundamental frequency gives toroidal mode number $n = +2$ (higher harmonics are also visible in the spectrogram, which may be either "spatial harmonics" in the island structure or "temporal harmonics" due to non-uniform island rotation), where positive mode number indicate propagation in the ion diamagnetic drift direction,

due to the residual rotation associated to neutral beam injection. Unfortunately the estimation of the poloidal mode number m from Mirnov coils would require a greater coverage of the poloidal angle, so various poloidal mode numbers are possible, up to $m = 7$, taking into account that the edge safety factor q_{95} is changing from 3.4 to 3.7 in the time interval considered in the figure. A continuous increase in the mode amplitude and a continuous decrease in the mode frequency are observed after the NBI power switch-off. An approximately constant frequency (below 1 kHz) is observed after 13.75 s, but mode analysis gives toroidal mode number $n = -2$, indicating propagation in the "natural" electron diamagnetic drift direction. This means that the island velocity has changed sign, with a frequency value passed through zero following the NBI switching-off. In addition to oscillations associated with TM activity, the MHD spectroscopy reveals other components, around 13 kHz (B1) and 10 kHz (B2), that accompany the development of TM activity. It is worth noting that the time traces of the electron temperature contours from electron cyclotron emission (ECE) radiometry, reported in figure 2 (right), show the simultaneous presence of magnetic islands at two different locations: $R = 3.58$ m (corresponding approximately to $q = 3/2$ resonant surface) and $R = 3.71$ m (corresponding to $q = 5/2$), respectively, but rotating with the same velocity along the toroidal direction. The hypothesis we would like to evaluate is that the additional components B1 and B2 in the spectrogram are two different BAEs (nay two different pairs of BAEs) associated with the two different magnetic islands 3/2 and 5/2, respectively.

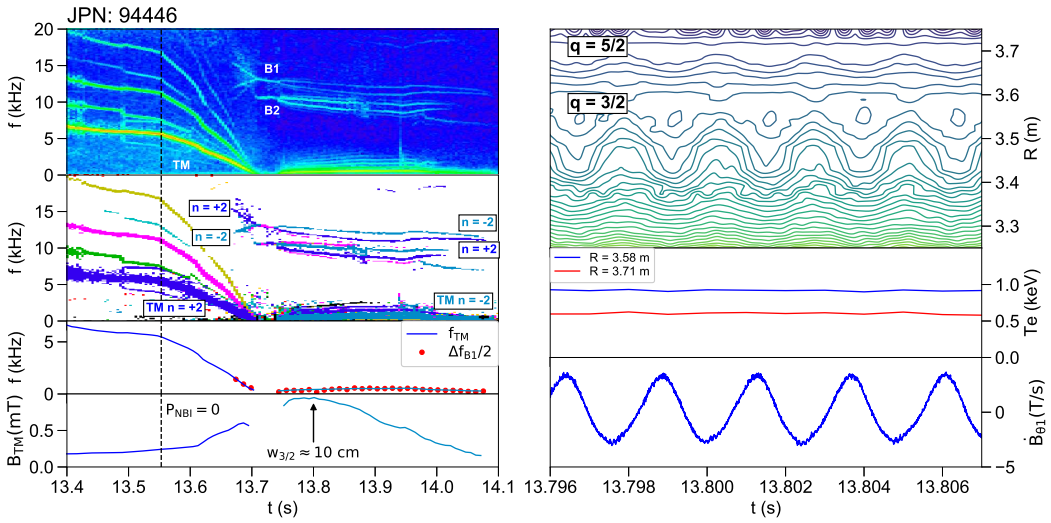

Figure 2. (Left) From top to bottom: spectrogram from a Mirnov coil; toroidal mode number analysis from an array of Mirnov coils; $|n| = 2$ TM frequency (solid line), compared with the half difference between the frequencies of two branches of oscillations around 13 kHz (solid circles); $|n| = 2$ TM amplitude from Mirnov coils. (Right) From top to bottom: electron temperature contours from ECE radiometry; electron temperatures at the islands location from ECE measurements; derivative of the poloidal magnetic field perturbation from a Mirnov coil. JPN 94446.

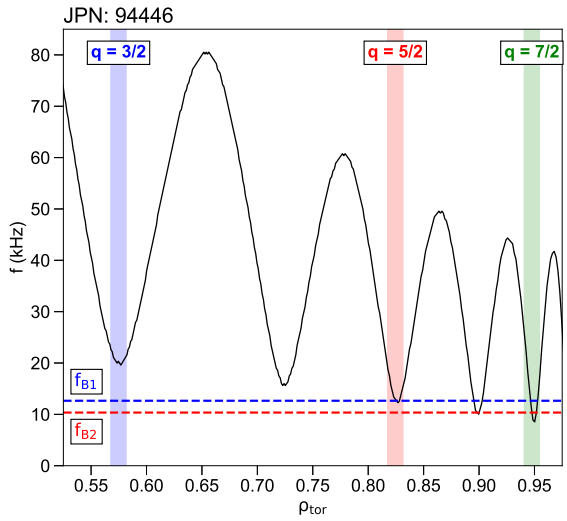

Figure 3. The $n = 2$ Alfvén continuum calculated by FALCON code for JPN 94446 at 13.74 s. The experimental frequencies B1 and B2 are reported as blue and red dashed lines, respectively.

As a first remark, the observed spectrogram is very similar to the ones associated with BAE in many other works [13, 15, 16, 17] and the frequency values fall in the BAE frequency range. In fact, assuming $T_i \approx T_e$ in equation (3) (with $R_0 \approx 3$ m) and considering the temperature values at the islands location on $q = 3/2$ and $q = 5/2$ resonant surfaces, frequency values of the order of 25 kHz and 20 kHz, respectively, are obtained for $\omega_{CAP}/2\pi$ between 13.70 s and 13.75 s. If we assume that the component B1 (13 kHz) is associated with the magnetic island 3/2 and the component B2 (10 kHz) is associated with the magnetic island 5/2, we can conclude that the components B1 and B2 fall in the respective beta-induced gaps ($\alpha \approx 0.5$ in equation (4)). These observations support the hypothesis that BAE oscillations at different frequencies are associated with magnetic islands located on different resonant surfaces, with the values of the BAE frequencies related to the temperature at the different island locations through equations (3) and (4). In order to support the interpretation of the observed oscillations as BAE, the $n = 2$ Alfvén continuum has been calculated by FALCON code [28], starting from the reconstructed equilibrium and the density profile for JPN 94446 at 13.74 s and the ideal MHD results have been re-scaled to account for kinetic effects. The black line in figure 3 denotes the $n = 2$ Alfvén continuum, where the accumulation frequency is about 19.9 kHz and 12.6 kHz for the resonant surfaces 3/2 and 5/2, respectively. Hence, the experimental frequencies B1 and B2, marked by blue and red dashed lines and assumed to be associated with magnetic islands on resonant surfaces 3/2 and 5/2, respectively, are consistent with the frequency gaps of BAE continuum. The possibility that the two components B1 and B2 are associated with another pair of islands, i.e. 5/2 and 7/2, cannot be ruled out, also taking into account the difficulty of obtaining accurate profiles in the presence of hollow temperature profiles. It has been found

that the experimental BAE frequencies measured in many pulses scale linearly with the frequency of the continuum accumulation point in agreement with equations (3) and (4), as observed also in the other devices mentioned before. A systematic comparison between the experimental frequencies and the ones calculated by FALCON code over a large dataset of pulses will be reported in future works.

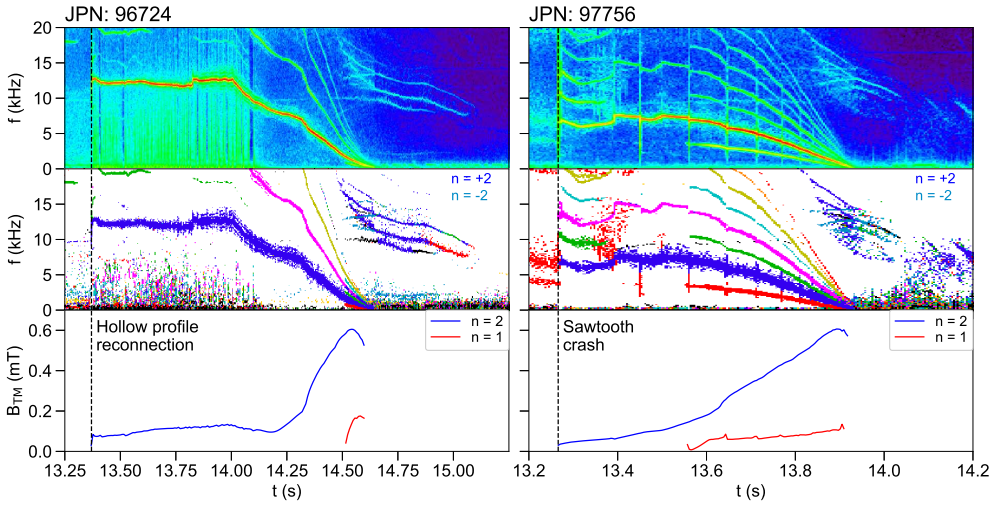

Figure 4. From top to bottom: spectrogram from a Mirnov coil; toroidal mode number analysis from an array of Mirnov coils; $n = +2$ (blue line) and $n = +1$ (red line) TM amplitude from Mirnov coils. JPN 96724 (left), JPN 97756 (right).

Another important point in support of the hypothesis of BAE associated with TM is that in the phases in which the islands are rotating at higher frequencies the oscillations centered around 13 kHz and 10 kHz, respectively, are split in two branches with opposite toroidal mode numbers (figure 2, left). The higher frequency branch has the same toroidal mode number as the TM (co-rotation with TM), whilst the lower frequency branch has the opposite toroidal mode number (counter-rotation with TM). This property is verified both in the ion rotation phase and in the electron one. In addition, the frequency difference Δf_B between each pair of branches is exactly twice the fundamental frequency of island oscillations f_{TM}, namely $\Delta f_B \equiv f_{B,Co} - f_{B,Cn} = 2f_{TM}$, so each pair of branches corresponds to two counter-propagating BAEs (referred as "twin BAEs" in the following) forming a "standing waves" in the island rest frame, with frequency $f_B \equiv (f_{B,Co} + f_{B,Cn})/2$, and the frequency difference between the two branches can be accounted for by the Doppler shift in the laboratory system:

$$f_{B,Co/Cn} = f_B \pm f_{TM} \tag{5}$$

When the islands are rotating at very low frequencies, from 13.70 s to 13.75 s, the two branches degenerate in a single line given by the overlapping of the two counter-propagating waves. These observations are recurrent in all works about BAE in the presence of magnetic islands and they have been verified over many pulses on JET.

The last point we would like to discuss concerns the existence of a threshold on TM amplitude for BAE excitation. The temporal evolution of the $|n| = 2$ TM amplitude is reported for JPN 94446 in figure 2 (left), showing an increase from 13.6 s and 13.8 s (a maximum island with of the order of 10 cm is inferred from the electron temperature contours for the 3/2 TM), followed by a progressive decrease up to the mode stabilization. The correlated appearance and disappearance of BAE seems indicate that a critical TM amplitude is necessary for excitation of the BAE (although such a threshold could depend on various properties of the thermal plasma), which is in accordance with the need to have magnetic islands sufficiently large to transfer enough energy to BAE to overcome Landau damping. The existence of a minimum TM amplitude to excite BAE has been verified over many pulses on JET. As additional examples, two pulses with $n = +2$ TM triggered by a reconnection process are reported in figure 4, and the excitation of multiple $n = \pm 2$ BAE is observed when the TM amplitude exceeds 0.5 mT. The excitation of BAE with $n = 2$ is reported for the first time in this work, whilst all the observations reported in the previous works concerned BAE with $n = 1$, which will be discussed in the next section.

4. Excitation of BAE with toroidal number $n = 1$

Time traces of some relevant quantities for a pulse (JPN 97589) characterized by a temperature hollowing after the reduction of the neutral beam injection and by the linear destabilization of a $n = +1$ TM with frequency around 3 kHz are reported in figure 5 (left). After a reconnection event at 14.56 s, the island rotation slows down, as visible from Mirnov and saddle coils, and the mode starts to slowly rotate in the electron diamagnetic drift direction ($n = -1$). Afterwards, a new reconnection event at 15.03 s leads to mode locking. In addition to oscillations associated with TM activity, the spectrogram reveals multiple components, between 8 kHz and 20 kHz, that accompany the development of TM activity. In the first phase two components are more visible, around 17 kHz (B1) and 13 kHz (B2), respectively; a third component, around 11 kHz (B3) is barely visible in the spectrogram, although its intensity increases after the reconnection event at 15.03 s. Also in this case the hypothesis we would like to evaluate is that these additional components in the spectrogram (B1, B2, B3) are different BAEs (nay twin BAEs) associated with different magnetic islands.

To investigate the simultaneous presence of magnetic islands on different rational surfaces, the time traces of the electron temperature contours from ECE radiometry have been reported in figure 6 (left), highlighting the presence of magnetic islands at three different locations, $R = 3.43$ m, $R = 3.62$ m, and $R = 3.73$ m, respectively, as confirmed by the local flattening in the electron temperature profile corresponding to the island O-point with respect to the island X-point (figure 6, right). The radii of the three flattening regions are in a good agreement with the position of the resonant surfaces corresponding to $q = 2$, $q = 3$ and $q = 4$, as estimated by the equilibrium safety factor profile with magnetic and pressure constraints, despite the difficulty of obtaining accurate

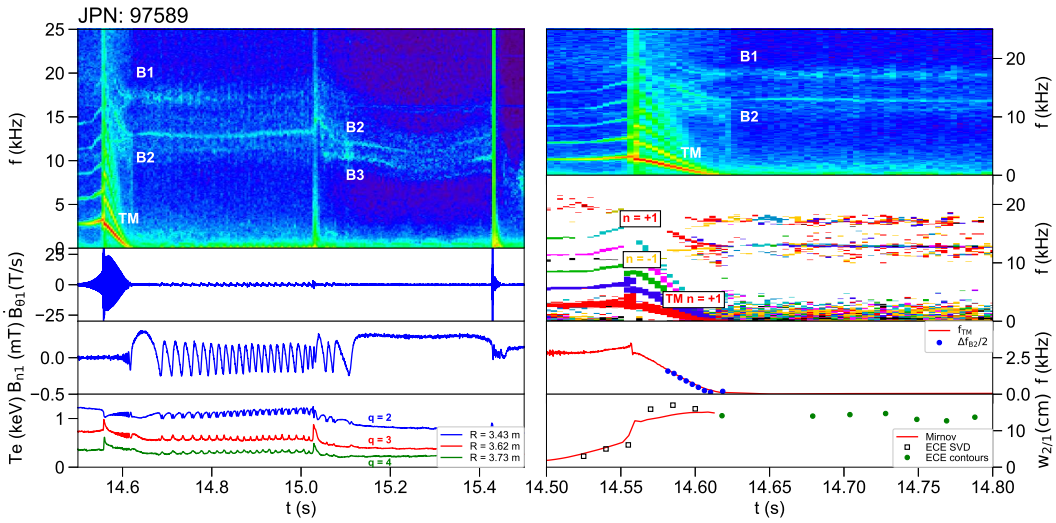

Figure 5. (Left) From top to bottom: spectrogram from a Mirnov coil; derivative of the poloidal magnetic perturbation from a Mirnov coil; $|n| = 1$ sine component on saddle coils; electron temperature at the islands location. (Right) From top to bottom: spectrogram from a Mirnov coil; toroidal mode number analysis from an array of Mirnov coils; $|n| = 1$ TM frequency (solid line), compared with the half difference between the frequencies of two branches of oscillations around 13 kHz (solid circles); 2/1 island width from Mirnov coils (solid line), SVD analysis of ECE channels (open squares) and ECE contours (solid circles). JPN 97589.

safety factor profiles in the presence of hollow temperature profiles. These observations reinforce the hypothesis that the additional components in the spectrogram at different frequencies could be different BAEs associated with magnetic islands located on different resonant surfaces (2/1, 3/1 and 4/1), but rotating with the same toroidal velocity, with the values of the BAE frequencies related to the temperatures on the respective resonant surface through equations (3) and (4). As a first check, the observed frequency values fall in the BAE frequency range. In fact, assuming $T_i \approx T_e$ in equation (3) and considering the temperature values at the islands location on $q = 2/1$, $q = 3/1$ and $q = 4/1$ resonant surfaces, the upper bound frequencies $\omega_{CAP}/2\pi$ between 14.65 s and 14.80 s result to be 28 kHz, 21 kHz and 17 kHz, respectively. If we assume that the component B1 (17 kHz) is associated with the magnetic island 2/1, the component B2 (13 kHz) with the island 3/1 and the component B3 (11 kHz, also if barely visible) with the island 4/1, we can conclude that the components B1, B2 and B3 fall in the respective beta-induced gaps ($\alpha \approx 0.6$ in equation (4)). In addition to the general agreement between the observed BAE frequencies and the ones predicted at a first glance by equations (3) and (4), the correspondence between frequencies and temperatures variations found even in the case of blips due to small reconnection events (as visible in figure 5 (left) for JPN 97589 at 15.03 s), supports the hypothesis that BAE oscillations at different frequencies could be associated with magnetic islands on different resonant surfaces.

To continue the verification of the standard features associated with BAE in

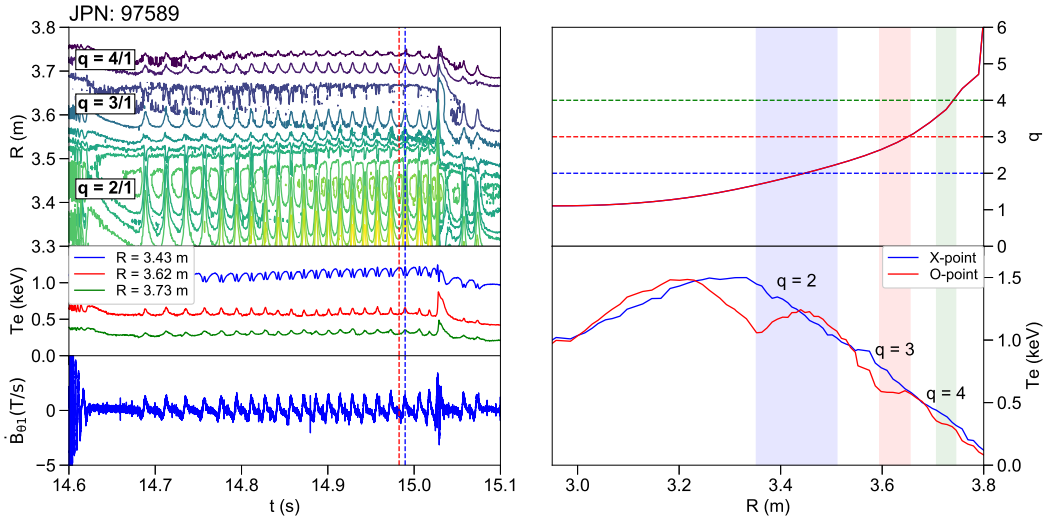

Figure 6. (Left) From top to bottom: electron temperature contours from ECE radiometry; electron temperature at the islands location; derivative of the poloidal magnetic field perturbation from a Mirnov coil. (Right) From top to bottom: equilibrium safety factor profile with magnetic and pressure constraints; electron temperature profile corresponding to the island O-point and X-point indicated on the left with vertical dashed lines. The electron temperature profile is hollow, with the maximum far off the magnetic axis located around 2.95 m. JPN 97589.

presence of large magnetic islands, a more detailed analysis of JPN 97589 is reported in figure 5 (right). The analysis of each pair of branches observed in the BAE frequency range before the mode locking (at 17 kHz and 13 kHz, respectively) confirms an opposite toroidal mode number $n = \pm 1$, with the same toroidal mode number as the TM ($n = +1$) for the higher frequency branch (co-rotation with TM), an opposite toroidal mode number ($n = -1$) for the lower frequency branch (counter-rotation with TM) and a frequency difference between each pair of branches exactly twice the fundamental frequency of TM oscillations. When the TM is locked the two branches degenerate in a single line given by the overlapping of the two counter-propagating waves. Finally, the evolution of the 2/1 island width has been estimated by singular value decomposition (SVD) [41] analysis of electron temperature fluctuations (ECE channels acquired at 200 kHz), highlighting a sudden transition from 6 cm to 16 cm after the reconnection event at 14.56 s. The island growth is confirmed by the rough estimate from the poloidal magnetic perturbations measured by Mirnov coils ($w \propto \sqrt{\dot{B}_{\theta 1}/f_{TM}}$ [42]), with a normalization on the SVD estimate (to take into account the fact that the Mirnov signal contains the contribution from different islands), and by a direct estimate from ECE contours when the island is slowly rotating. The observation of BAE oscillations only after the transition to larger island widths supports the hypothesis of a threshold effect on TM amplitude for BAE excitation, so we can conclude that BAE cannot be driven when the island width remains below a certain threshold.

As additional examples of the existence of a critical magnetic island size for BAE

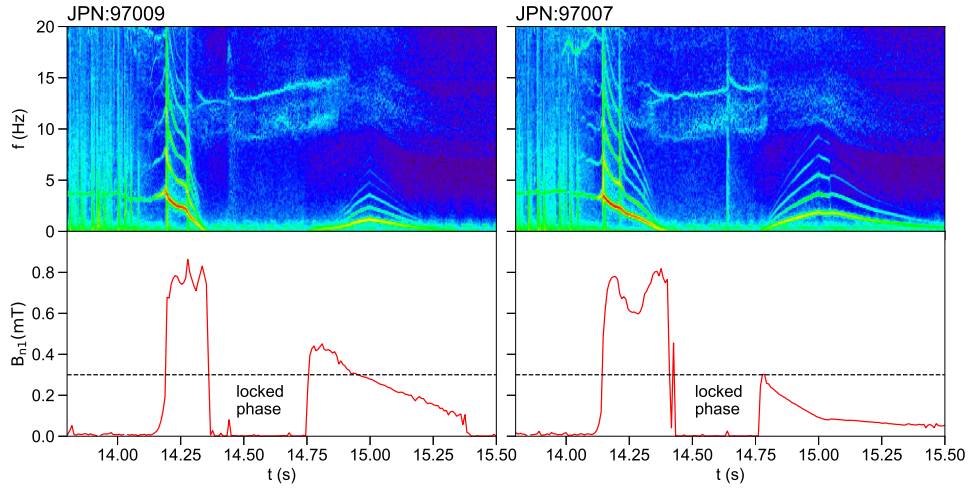

Figure 7. From top to bottom: spectrogram from a Mirnov coil; $|n| = 1$ TM amplitude from Mirnov coils. JPN 97009 (left), JPN 97007 (right).

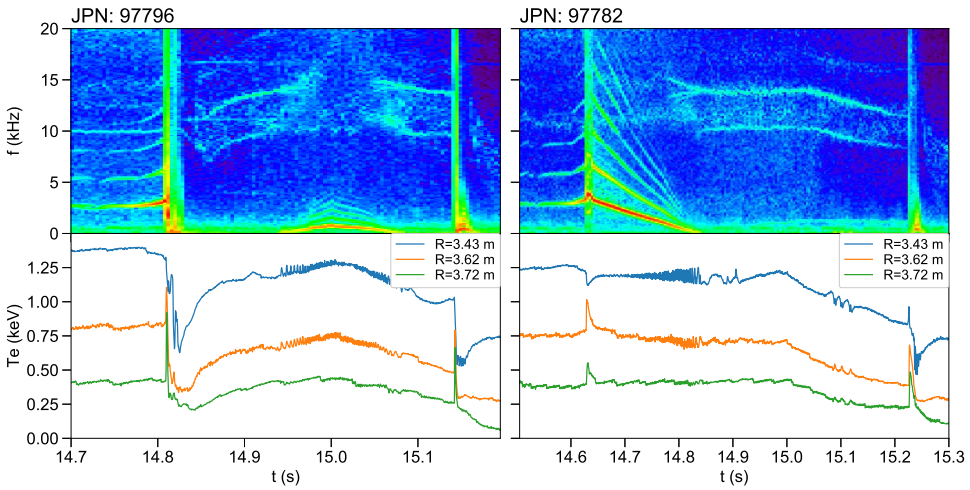

Figure 8. From top to bottom: spectrogram from a Mirnov coil; electron temperature at the islands location evaluated by ECE contours. JPN 97796 (left), JPN 97782 (right).

excitation, two pulses with $|n| = 1$ TM are reported in figure 7, and the excitation of $|n| = 1$ BAE is observed after an increase in TM amplitude, while BAE disappear when the TM amplitude reduces below 0.3 mT. This behavior has been observed in several JET pulses, indicating that a critical size for the magnetic island has to be exceeded for BAE excitation, even if the exact value for the threshold could depend on different plasma properties (e.g. the safety factor profile). This phenomenon is similar to the results observed on FTU [13], HL-2A [16] and J-TEXT [17]. As additional examples of the general scaling of the BAE frequencies with the plasma temperature at the islands location, two pulses with $|n| = 1$ TM are reported in figure 8, where it is possible

to see that BAE frequencies generally follow the island temperature evolutions due to the change of the electron temperature profile even if additional parameters influencing BAE frequencies should be taken into account (e.g. the safety factor profile). This general trend has been observed in different pulses on JET and on other tokamaks. The pulses shown so far and the considerations made are representative of the general chain of events leading to the onset of BAE, but clearly they not catch all the possible behaviors. As an example, multiple BAE oscillations with $n = 1$ are usually observed in the hybrid scenario with higher q_{95} values and hollow temperature profiles. On the contrary, multiple BAE oscillations with $n = 2$ are observed both in the hybrid scenario and baseline, and the trigger for TM onset or enhancement can be either a sawtooth crash in peaked temperature profiles or a reconnection event in hollow temperature profiles.

5. BAE and GAM excitation in the landing phase

Long lasting oscillations between 5 kHz and 20 kHz are sometimes observed in the landing phase of JET pulses (figure 9). All these pulses are characterized by TM signals on the saddle coils, so these oscillations could be explained in terms of BAE and GAM associated with locked or slowly rotating TM, as suggested in section 2 for JPN 94446.

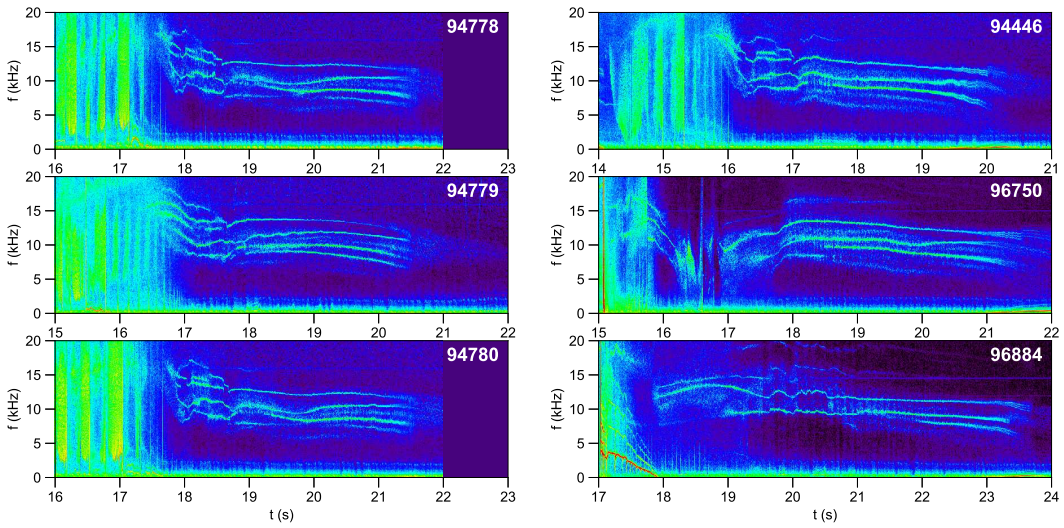

Figure 9. Spectrogram of the landing phase of JET pulses from Mirnov coils. All pulses are characterized by locked or slowly rotating tearing modes.

To support the hypothesis of a strong correlation among TM, BAE and GAM, the landing phase of JPN 97770 is reported in figure 10 (left). In this pulse TM activity with toroidal mode number $n = +1$ (rotation in the ion diamagnetic drift direction) is observed in the spectrogram from Mirnov coils at low frequencies after a reconnection event around 10.1 s and locked or slowly rotating tearing modes are observed after 10.3 s

in the saddle coils, with the corresponding appearance of long lasting oscillations in the BAE/GAM range between 5 kHz and 20 kHz. As a first remark, the hypothesis that BAE oscillations at different frequencies could be associated with magnetic islands on different resonant surfaces is supported by the time traces of the electron temperature contours from ECE radiometry reported in figure 11 (left) around $t = 10.5$ s, highlighting the presence of magnetic islands at different locations, but rotating with the same velocity along the toroidal direction. The presence of multiple islands is confirmed by the local flattening in the electron temperature profile corresponding to the island O-point with respect to the island X-point (figure 11, right). The radii of the four flattening regions are in a good enough agreement with the position of the resonant surfaces corresponding to $q = 2$, $q = 3$ $q = 4$, and $q = 5$ as estimated by the equilibrium safety factor profile. It is worth noting that in the landing phase temperatures at a given radius decrease over time due to the decrease in the heating power, whilst the radii of the resonant surfaces move inwards due to the increase in the edge safety factor. The combination of the two effects can help explain why the frequencies of BAE, linked to the temperature on the resonant surfaces, do not progressively decrease over time. Another interesting aspect is the possibility to use the BAE activity as indication of the presence of multiple locked or slowly rotating magnetic islands when the magnetic measurements are no longer available (as sometimes happens in the termination phase) or when the islands rotate with the same toroidal velocity and it is difficult to distinguish different modes having the same toroidal mode number. In the final stage of JPN 97770 (figure 10), after $t = 13.8$ s, the islands start to rotate faster, with Mirnov signal characterized by a toroidal mode number $n = -1$ (rotation in the electron diamagnetic drift direction), and all the BAE oscillations split in pairs of branches with opposite toroidal mode numbers, with $n = -1$ for the higher frequency branch (co-rotation with TM) and $n = +1$ for the lower frequency branch (counter-rotation with TM). In addition, the frequency difference between each pair of branches is exactly twice the fundamental frequency of island oscillations. It is worth noting that an additional component at the exact middle frequency between each pair of BAE branches and with $n = 0$ is also detected. Our hypothesis is that these additional fluctuations are GAM. This hypothesis is primarily supported by the fact that BAE and GAM have similar dispersion relations in the case of the long wavelength limit, namely the kinetic expression of the GAM dispersion relation can degenerate with that of the BAE [27]. A possible excitation mechanism of GAM in our pulse could be the non-linear interaction (i.e., three wave resonance) among GAM, BAE and strong TM. This hypothesis is reinforced by the threshold effect observed between 14.2 s and 14.5 s, when more diffuse BAE and GAM components are observed in the spectrogram in correspondence with a decrease in the TM amplitude (figure 10, right).

The appearance of multiple "triplets" in the spectrogram (twin BAEs plus GAM) is characteristic of the landing phase of pulses where the islands start to rotate faster. As additional examples, time traces of the landing phase of JPN 94446 and JPN 89074 are reported in figure 12 and figure 13, respectively. In both pulses, the long lasting

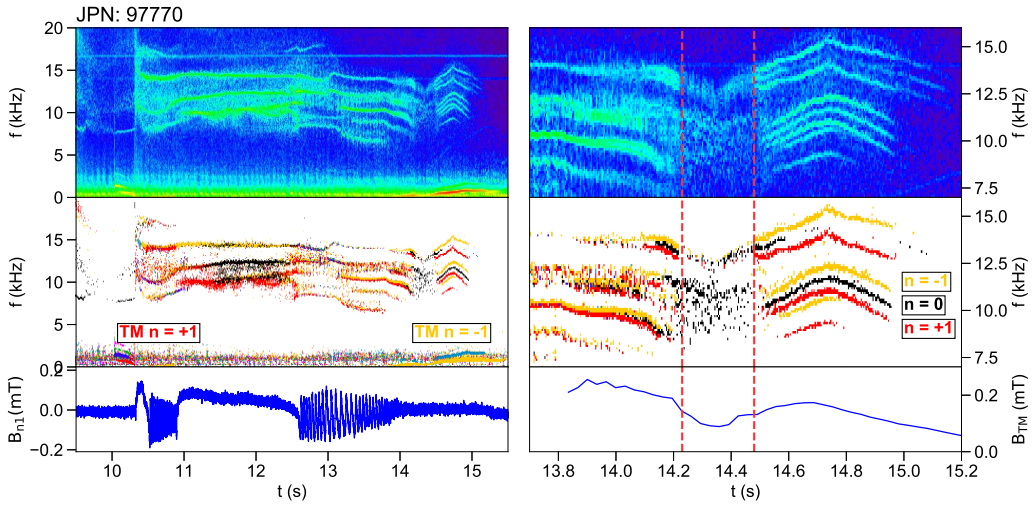

Figure 10. (Left) From top to bottom: spectrogram from a Mirnov coil; toroidal mode number analysis from an array of Mirnov coils, highlithing a change in the mode rotation from ion ($n = +1$) to electron ($n = -1$) diamagnetic drift direction; $|n| = 1$ sine component on saddle coils. (Right) From top to bottom: spectrogram from a Mirnov coil; toroidal mode number analysis from an array of Mirnov coils; mode amplitude from Mirnov coils. JPN 97770.

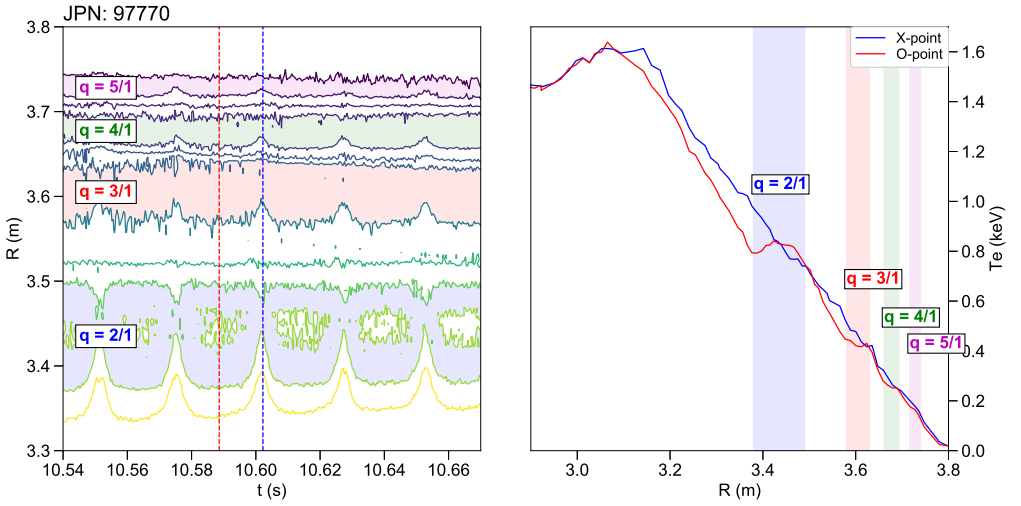

Figure 11. (Left) Electron temperature contours from ECE radiometry. (Right) Electron temperature profile corresponding to the island O-point and X-point indicated on the left with vertical dashed lines. JPN 97770.

oscillations between 5 kHz and 15 kHz are observed in the presence of slowly rotating tearing modes, as shown by signals of $|n| = 1$ sine component on saddle coils (figure 12 and figure 13, left). A toroidal mode number analysis is possible in the final stage (figure 12 and figure 13, right), when a faster TM rotation is recovered, characterized by $n = -1$, and three triplets (each composed by a pair of branches with $n = \pm 1$ and

a component with $n = 0$ at the exact middle frequency between each pair of $n = \pm 1$ branches) are observed at different frequencies, supporting the hypothesis that these long lasting oscillations are BAE and GAM associated with TM.

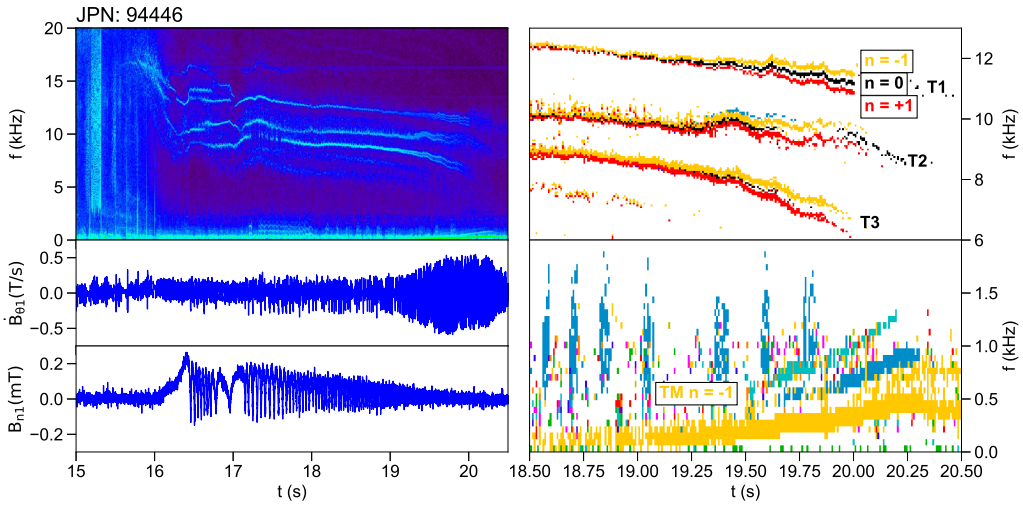

Figure 12. (Left) From top to bottom: spectrogram from a Mirnov coil; derivative of the poloidal magnetic perturbation from a Mirnov coil; $|n| = 1$ sine component on saddle coils. (Right) Toroidal mode number analysis for the final stage of termination in two different frequency range. JPN 94446.

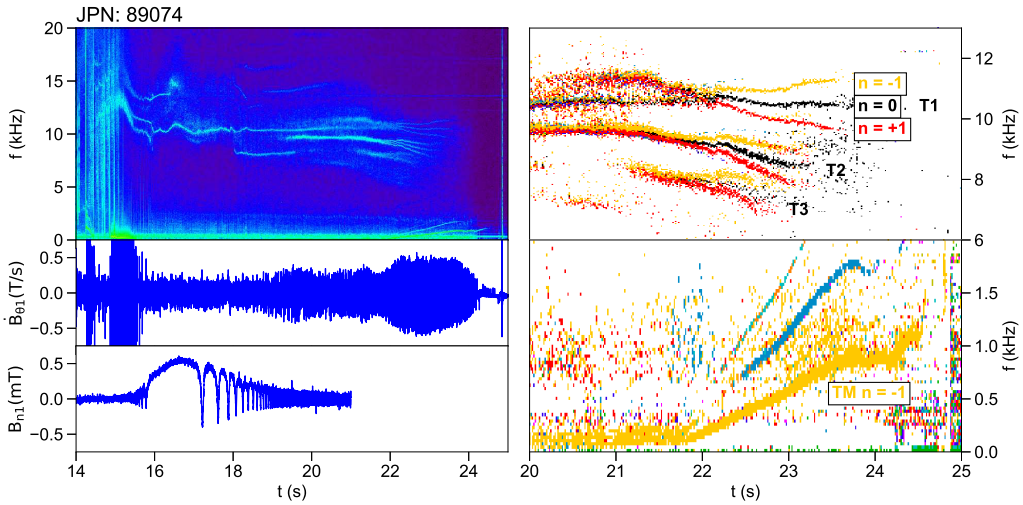

Figure 13. (Left) From top to bottom: spectrogram from a Mirnov coil; derivative of the poloidal magnetic perturbation from a Mirnov coil; $|n| = 1$ sine component on saddle coils. (Right) Toroidal mode number analysis for the final stage of termination in two different frequency range. JPN 89074.

A crossed spectral bi-coherence analysis of magnetic fluctuations associated with TM, BAE and GAM has been carried-out to verify the non-linear interaction among

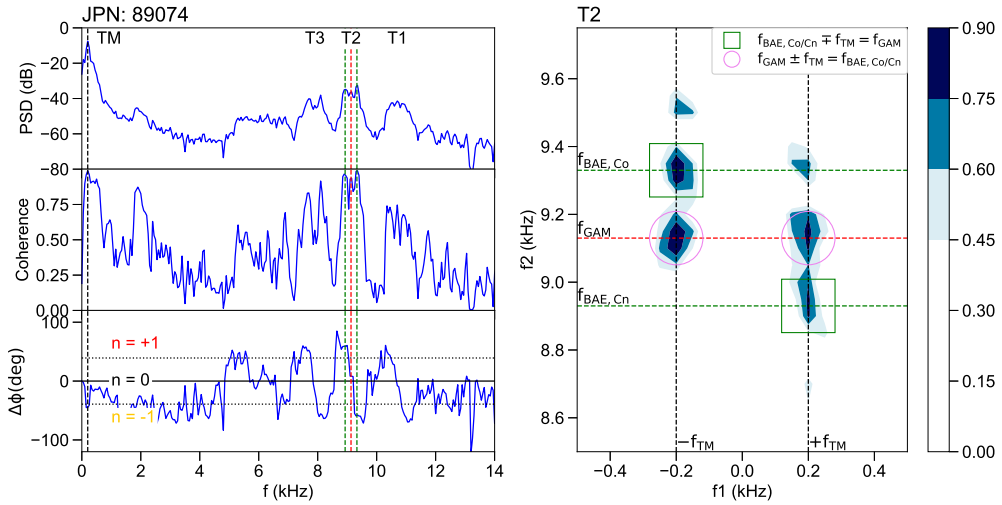

Figure 14. (Left) From top to bottom: crossed power spectral density; coherence; phase difference. (Right) Crossed bicoherence. JPN 89074 ($t = 22.1$ s).

the three modes, evaluating the degree of phase coherence between their fluctuations. Signals from two magnetic pick-up coils positioned at different toroidal angles have been utilized for the analysis and the results for JPN 89074 are reported in figure 14. The crossed power spectral density on the top left panel highlight the presence of TM activity around 0.2 kHz and three triplet centered around 10.7 kHz (T1), 9.2 kHz (T2) and 7.9 kHz (T3), respectively. High coherence values are obtained in correspondence of the three triplets (central panel) and for each triplet the analysis of the phase difference between the two selected coils (bottom panel) confirms the values of the toroidal mode numbers for the twin BAEs ($n = \pm 1$) and for the GAM ($n = 0$). The crossed bicoherence spectrum of magnetic fluctuations associated with TM, BAE and GAM is reported for triplet T2 on the right figure, showing strong non-linear interaction among those modes. We have to point out here that the direction of wave energy transfer in the non-linear interaction among TM, twin BAEs and GAM in unknown, and it needs to be assessed. If we suppose that GAM are excited by the non-linear interaction among twin BAEs and TM and we consider only the fundamental frequencies of those modes, the following matching condition have to be satisfied among those modes:

$$\begin{cases} f_{GAM} = f_{BAE,Cn} + f_{TM} \\ f_{GAM} = f_{BAE,Co} - f_{TM} \end{cases} \tag{6}$$

with the same kind of constraints posed on the toroidal mode numbers of the modes. These non-linear interaction relations correspond to the two green squares in the crossed bicoherence spectrum reported in figure 14 (right). However, also the following non-linear interaction relations are possible:

$$\begin{cases} f_{BAE,Co} = f_{GAM} + f_{TM} \\ f_{BAE,Cn} = f_{GAM} - f_{TM} \end{cases} \tag{7}$$

corresponding to the excitation mechanism where the twin BAEs are generated from the localized interaction between GAM and magnetic islands [43]. These non-linear interaction relations correspond to the two violet circles in the crossed bicoherence spectrum reported in figure 14 (right). In principle, the two different excitation mechanisms (i.e. $BAE + TM \Rightarrow GAM$ and $GAM + TM \Rightarrow BAE$) are not in conflict with each other. The possibility to obtain additional information combining electrostatic and magnetic features for GAM will be explored in near future.

6. Conclusions and Discussion

Magnetic oscillations in the range from 5 kHz to 20 kHz have been observed in the magnetic spectrogram of JET pulses without any fast particles population, characterized by strong tearing activity at lower frequencies. The experimental frequencies of such additional oscillations fall within the low-frequency gap opened, in the shear Alfvén continuous spectrum, by finite beta effects, suggesting that the observed modes are BAE. The simulation of a real pulse with a MHD code has been carried out to support that hypothesis. It is shown that, in presence of large rotating magnetic islands with toroidal mode number $|n| = 1$ or $|n| = 2$, BAE appear in pair of modes propagating in the opposite directions and forming a standing wave structure in the island rest frame. Therefore a possible explanation for BAE excitation is that pairs of counter-propagating BAE interact via three wave coupling with the magnetic island and are excited when the energy transfer rate from the island to the BAE is sufficient to overcome the Landau damping, which is in agreement with the experimental observation of an amplitude threshold of the magnetic island to be exceeded for effective BAE excitation.

It is worth noting that the observation of BAE with $n = \pm 2$ is reported for the first time in this work, with the analysis of several pulses, including a particular pulse where the island rotation changes from ion ($n = +2$) to electron ($n = -2$) diamagnetic drift direction, with the subsequent change in the toroidal mode number of co-rotating and counter-rotating BAE. As another novelty compared to previous works, the simultaneous presence of magnetic islands on different rational surfaces, rotating with the same toroidal velocity, has been highlighted in pulses with multiple oscillations in the BAE range. This observation supports the hypothesis that BAE oscillations at different frequencies could be associated with magnetic islands on different resonant surfaces, with the values of the BAE frequencies related to the temperatures at the islands location, in agreement with theoretical predictions based on the estimate of the accumulation point of the Alfvén continuous spectrum in the fluid limit.

The occurrence of multiple oscillations at different frequencies is observed also in the landing phase of plasma pulses with locked or slowly rotating modes. It is worth noting that in the final stage of the landing phase the edge safety factor is relatively high, so several relevant rational surfaces are present inside the plasma and different m/n TM can be destabilized, in agreement with the experimental observation of the simultaneous presence of magnetic islands on different rational surfaces, so many BAE oscillations can

be excited. In particular, the increase with m^2 of the line bending stabilization effect for TM and the decrease with $(m/n)^2$ of the Landau damping for BAE could help to explain why only BAE with the lowest toroidal mode numbers $n = 1, 2$ have been observed so far. Finally, pulses characterized by slowly rotating TM in the landing phase exhibit additional oscillations at the exact middle frequency between the two BAE branches and with toroidal mode number $n = 0$, likely associated with GAM, in agreement with the theoretical prediction of BAE/GAM degeneracy in the long-wavelength limit. A crossed bicoherence analysis has confirmed the non-linear interaction among geodesic acoustic modes, beta-induced Alfvén eigenmodes and tearing modes, although additional analysis are necessary to assess the direction of wave energy transfer in the non-linear interaction.

Acknowledgments

This work has been carried out within the framework of the EUROfusion Consortium and has received funding from the Euratom research and training programme 2014-2018 and 2019-2020 under grant agreement No 633053. The views and opinions expressed herein do not necessarily reflect those of the European Commission.

References

[1] Chu M S *et al* 1992 *Phys. Fluids* **B 4** 3713
[2] Turnbull A D *et al* 1993 *Phys. Fluids* **B 5** 2546
[3] Zonca F, Chen L and Santoro R A 1996 *Plasma Phys. Control. Fusion* **38** 2011
[4] Chen L and Zonca F 1995 *Phys. Scr.* **T60** 81
[5] King L W 1999 *Plasma Phys. Control. Fusion* **41** R1
[6] Cheng C Z, Chen L, Chance M S 1985 *Ann. Phys.* **161** 21
[7] Heidbrink W W *et al* 1993 *Phys. Rev. Lett.* **71** 855
[8] Nazikian R *et al* 1996 *Phys. Plasmas* **3** 593
[9] Nguyen C *et al* 2009 *Plasma Phys. Control. Fusion* **51** 095002
[10] Hole M J *et al* 2013 *Plasma Phys. Control. Fusion* **55** 045004
[11] Xu M *et al* 2013 *Plasma Phys. Control. Fusion* **55** 065002
[12] Furth H P, Killeen J, Rosenbluth M N 1963 *Phys. Fluids* **6** 459
[13] Buratti P *et al* 2005 *Nucl. Fusion* **45** 1446
[14] Annibaldi S V, Zonca F and Buratti P 2007 *Plasma Phys. Control. Fusion* **49** 475
[15] Zimmermann O *et al* 2005 *Proc. 32nd EPS Conf. on Plasma Physics and Controlled Fusion (Montreaux, Switzerland)* **D5.016**
[16] Chen W *et al* 2011 *Nucl. Fusion* **51** 063010
[17] Liu L *et al* 2015 *Plasma Phys. Control. Fusion* **57** 065007
[18] Winsor N, Johnson J L and Dawson J M 1968 *Phys. Fluids* **11** 2448
[19] Zhao K J *et al* 2006 *Phys. Rev. Lett.* **96** 255004
[20] Zonca F and Chen L 2008 *Europhysics Letters* **83** 35001
[21] Hasegawa A, Maclennan C G and Kodama Y 1979 *Phys. Fluids* **22** 2122
[22] Itoh K *et al* 2006 *Phys. Plasmas* **13** 055502
[23] Fujisawa A *et al* 2009 *Nucl. Fusion* **49** 013001
[24] Manz P, Ramisch M and Stroth U 2009 *Phys. Rev. Lett.* **103** 165004
[25] Berk II *et al* 2006 *Nucl. Fusion* **46** S888
[26] Boswell C J *et al* 2006 *Phys. Lett. A* **358** 154
[27] Zonca F, Briguglio S, Chen L *et al* 2006 *Plasma Phys. Control. Fusion* **48** B15
[28] Falessi M, Carlevaro N, Fusco V, Giovannozzi E, Lauber P, Vlad G and Zonca F 2020 *Journal of Plasma Physics* **86** (5) 845860501
[29] Chen W *et al* 2013 *Nucl. Fusion* **53** 113010
[30] Kim Y C and Powers E J 1979 *IEEE Trans. on Plasma Science* **2** (Vol. PS-7) 120
[31] Gerasimov S N *et al* 2020 *Nucl. Fusion* **60** 066028
[32] Joffrin E, Baruzzo M, Beurskens M, Bourdelle C, Brezinsek S, Bucalossi J, Buratti P, Calabrò G, Challis C D, Clever M, Coenen J, Delabie E, Dux R, Lomas P, de la Luna E, de Vries P, Flanagan J, Frassinetti L, Frigione D, Giroud C, Groth M, Hawkes N, Hobirk J, Lehnen M, Maddison G, Mailloux J, Maggi C F, Matthews G, Mayoral M, Meigs A, Neu R, Nunes I, Püetterich T, Rimini F, Sertoli M, Sieglin B, Sips A C C, van Rooij G, Voitsekhovitch I 2014 *Nucl. Fusion* **54** 013011
[33] Dux R, Neu R, Peeters A G, Pereverzev G, Mück A, Ryter F, Stober J 2003 *Plasma Phys. Controlled Fusion* **45** 1815
[34] Valisa M, Carraro L, Predebon I, Puiatti M E, Angioni C, Coffey I, Giroud C, Lauro Taroni L, Alper B, Baruzzo M, Belo daSilva P, Buratti P, Garzotti L, Van Eester D, Lerche E, Mantica P, Naulin V, Tala T, Tsalas M 2011 *Nucl. Fusion* **51** 033002
[35] McGuire K *et al* 1983 *Phys. Rev. Lett.* **50** 891
[36] Garzotti L, Challis C, Dumont R, Frigione D, Graves J, Lerche E, Mailloux J, Mantsinen M, Rimini F, Casson F, Czarnecka A, Eriksson J, Felton R, Frassinetti L, Gallart D, Garcia J, Giroud C, Joffrin E, Hyun-Tae Kim, Krawczyk N, Lennholm M, Lomas P, Lowry C, Meneses L, Nunes I, Roach C M, Romanelli M, Sharapov S, Silburn S, Sips A, Stefániková E, Tsalas M, Valcarcel

D, Valovic M 2019 *Nucl. Fusion* **59** 076037
[37] Hobirk J *et al* 2012 *Plasma Phys. Control. Fusion* **54** 095001
[38] de Vries P C, Baruzzo M, Hogeweij G M D, Jachmich S, Joffrin E, Lomas P J, Matthews G F, Murari A, Nunes I, Pütterich T, Reux C, Vega J 2014 *Phys. Plasmas* **21** 056101
[39] Hobirk J Hobirk J, Bernert M, Buratti P, Challis C D, Coffey I, Drewelow P, Joffrin E, Mailloux J, Nunes I, Pucella G, Pütterich T, de Vries P C 2018 *Nucl. Fusion* **58** 076027
[40] Pucella G *et al* 2021 *Nucl. Fusion* accepted for pubblication
[41] Nardone C 1992 *Plasma Phys. Controlled Fusion* **34** 1447
[42] Wesson J A 2004 *Tokamaks*, 3rd Edition, Oxford University Press
[43] Xu M *et al* 2020 *Nucl. Fusion* accepted for pubblication